Sparse-Aperture Adaptive Optics

Peter Tuthill[a], James Lloyd[b], Michael Ireland[c] Frantz Martinache[b], John Monnier[d], Henry Woodruff[a], Theo ten Brummelaar[e], Nils Turner[e], Charles Townes[f]

[a]School of Physics, University of Sydney, NSW 2006, Australia;
[b]Astronomy Department, Cornell University USA;
[c]Planetary Science, Caltech 1200 E. California Blvd, 150-21 Pasadena CA 91125, USA;
[d]Astronomy Department, Cornell University of Michigan USA;
[e]Center for High Angular Resolution Astronomy, GSU, Atalanta, GA 30303, USA
[f]Space Science Lab, U.C. Berkeley, CA 94720, USA

ABSTRACT

Aperture masking interferometry and Adaptive Optics (AO) are two of the competing technologies attempting to recover diffraction-limited performance from ground-based telescopes. However, there are good arguments that these techniques should be viewed as complementary, not competitive. Masking has been shown to deliver superior PSF calibration, rejection of atmospheric noise and robust recovery of phase information through the use of closure phases. However, this comes at the penalty of loss of flux at the mask, restricting the technique to bright targets. Adaptive optics, on the other hand, can reach a fainter class of objects but suffers from the difficulty of calibration of the PSF which can vary with observational parameters such as seeing, airmass and source brightness. Here we present results from a fusion of these two techniques: placing an aperture mask downstream of an AO system. The precision characterization of the PSF enabled by sparse-aperture interferometry can now be applied to deconvolution of AO images, recovering structure from the traditionally-difficult regime within the core of the AO-corrected transfer function. Results of this program from the Palomar and Keck adaptive optical systems are presented.

Keywords: Optical Interferometry, Adaptive Optics

1. INTRODUCTION AND PRINCIPLES

Despite considerable investment, much of the promise of adaptive optics (AO) to deliver diffraction-limited images has yet to be fully realized. This is largely due to difficulties imposed by the complicated, unstable, and unknown point-spread function (PSF). Sparse-Aperture AO addresses the problems of precise calibration and system characterization of AO systems by use of a novel application of aperture masking interferometry. Although the extraction of diffraction-limited structure from within the core of the AO-corrected PSF has ranked as one of the most intractable problems plaguing the field, the use of a non-redundant pupil mask (NRM), as we show later, ameliorates most of these difficulties. The combination of NRM with AO can lead not only to the precise calibration of structure delivered by the AO system up to the highest angular resolutions, it can also give the ability to push high-fidelity image recovery into the optical regime.

Although so far restricted to bright targets, many of the most precise high-resolution astronomical images have been made with highly filled Fourier data from non-redundant aperture masking interferometry. This high-fidelity of NRM data offers a solution to the problem of PSF characterization in AO imaging: synthesizing the heritage of image reconstruction with sparse pupil sampling from astronomical interferometry with the long coherence times available after AO correction. Marrying these two techniques will bring the precision calibration shown to come with sparse-aperture Fizeau-type interferometry together with extremely high dynamic range and the relatively faint target capability of AO.

In particular, the proven calibration advantages of NRM can be used to extend the capability of AO in a number of distinct ways: (1) higher fidelity imaging is possible in and around the core of the PSF; (2) the reach of AO may be pushed into into the visible part of the spectrum, a region where prior successes have been limited; and (3) novel system performance experiments studying the AO response can be enabled.

(Send correspondence to P.T. E-mail p.tuthill@physics.usyd.edu.au)

Advances in Adaptive Optics II, edited by Brent L. Ellerbroek, Domenico Bonaccini Calia,
Proc. of SPIE Vol. 6272, 62723A, (2006) · 0277-786X/06/$15 · doi: 10.1117/12.672342

1.1. The Nature of the AO PSF Problem

There are a number of reasons why AO systems have not yet achieved imaging at their fullest potential. For example, an AO system uses a wavefront sensor (WFS) with a finite number of sub-apertures, as well as a deformable mirror with a finite number of actuators, and this results in a finite spatial bandwidth. The atmospheric phase corruption nominally follows a Kolmogorov power law between the outer scale length of the turbulence and the molecular damping scale of the air, and this far exceeds the spatial bandwidth of any realizable AO system. Even a perfect AO system cannot correct the phase errors on scales smaller than the actuator spacing, resulting in leakage of high spatial frequency errors which are manifest as an uncorrected halo in the PSF. Similarly, the finite temporal bandwidth of the AO system results in additional leakage of uncorrected phase.

Another problem is that present generation systems do not sense the wavefront through the same optical path as the science observation, resulting in non-common path and AO system calibration errors. Furthermore, these errors couple into the dynamic correction through the dependence of the Shack-Hartmann wavefront sensor gain on seeing, resulting in continual fluctuation between over and under-correction of the non-common path errors.

The PSF of an AO system fluctuates on all timescales, and is also sensitively dependent on a multitude of parameters such as guide star brightness, seeing, airmass, and servo bandwidth. As a consequence, measurement of the PSF on a reference star for use in deconvolution or PSF subtraction of a subsequent science target has been fraught with difficulties. Controversy continues to surround the reality of structure reported in many systems.

Substantial progress has been made resolving this problem by exploiting simultaneous differential measurements in polarization[1–3] or wavelength.[4,5] These techniques are useful in cases where there is a large differential signal, but do not address the generic problem of the fidelity of adaptive optics imaging.

1.2. Non-Redundant Masking

The non-redundant masking technique[6] transforms the telescope into a sparse, separated-element array with a Fizeau-type beam combination scheme by the simple action of placing an apodizing plate over the pupil. It is instructive to examine the continuing success of this technique, which essentially dates back to Fizeau himself, in delivering unsurpassed image quality. When two or more pairs of coherent sub-apertures contribute to the same spatial frequency, that is they have the same baseline, then in a seeing-limited case, the power will add incoherently. The resultant baseline power will then be a random walk of R steps where R is the *redundancy* – the number of times the given baseline is repeated within the pupil. In the bright source limit, the noise inherent to this random walk process completely dominates the signal-to-noise (SNR), leading to the well-known result that the SNR of speckle frames saturates to 1. The success of NRM can then be easily visualized: in order to create a non-redundant array one must discard most of the pupil area, and so lose most of the signal, but one also removes *all of the atmospheric noise*, and this leads to dramatically enhanced SNR.

In cases where a target is bright enough to deliver adequate signal through the mask, this immunity to atmospheric noise leads to precisely calibrated complex visibility data. As an illustration, data from the highly successful Keck aperture masking experiment[7] which has been producing near-IR images for many years is depicted in Figure 1. The method of NRM is a solution to the ill-posed deconvolution of an unknown PSF from an unknown object. It does this by sampling the unknown object with a series of known PSFs, and applying constraints to the set of possible relative phases. The success of NRM also takes advantage of the concept of closure phase[8] which utilizes the summation of phases around closed triangles of baselines thereby allowing the estimation of relative phase structure in the target independent of the existence of atmospheric degradation. Reconstruction of the highest fidelity images, therefore, does not necessarily suffer from the penalty imposed by the loss of light at the non-redundant mask as one might naively assume. Indeed, the highest spatial frequency information on the longest baselines is largely preserved by NRM which preferentially culls the redundant shorter baselines in the aperture.

1.3. NRM with AO

Although NRM and AO have been treated as competing approaches, there are persuasive arguments that in combining the two one can preserve the relative strengths and ameliorate the relative weaknesses.

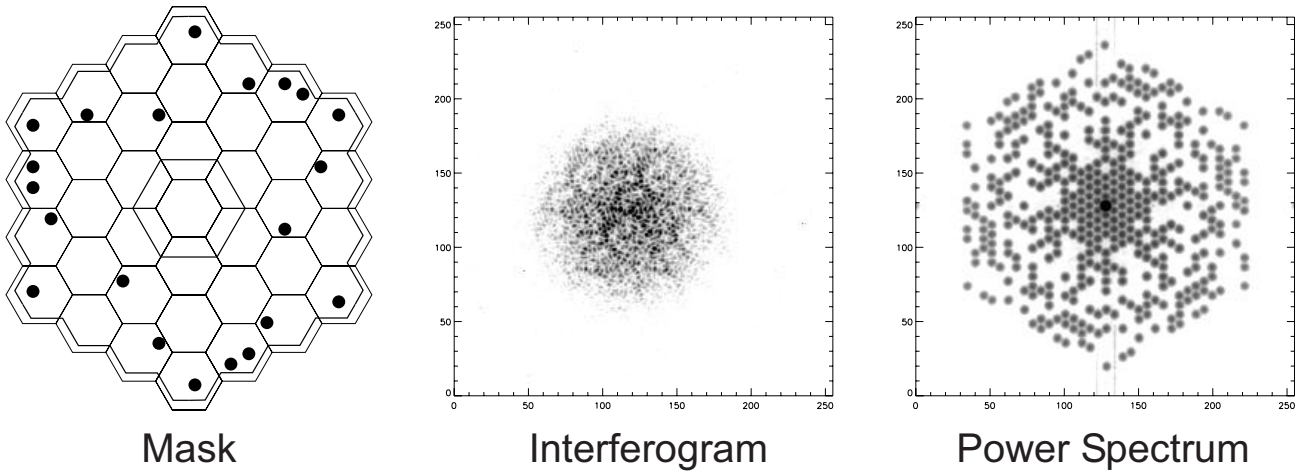

Figure 1. Keck aperture masking experiment with seeing limited data. The leftmost panel shows the non-redundant mask applied to the Keck telescope aperture. Light is only allowed to pass through 21 precisely located holes, each only 0.35 m diameter on the sky. The center panel shows a short exposure image (interferogram) of the fringe pattern produced by the mask. The right panel shows the averaged power spectrum of 100 frames, showing power on all 210 baselines. Note that the visibility in the longest baselines is attenuated due to atmospheric effects.

In addressing the AO PSF problem, it is instructive to return to our redundancy argument above. Behind a functioning AO system, spectral power is no longer a random walk of R steps as for the uncorrected case, but neither is it the coherent sum of R vectors unless the AO system is performing perfectly. The AO result, therefore, will be intermediate between these extremes, with both coherent and incoherent (random walk) components, proportionate to the efficacy of the AO correction. However, the essential point is that in the presence of a redundant pupil, there remains a random atmospheric noise component. This "speckle noise" component remains orders of magnitude larger than any other process degrading the AO PSF.[9,10] Fortunately, NRM will eliminate this noise process, just as it does for the non-AO case. In a non-redundant pupil, the fringes will have some phase jitter due to imperfect AO correction, but their amplitudes will be unaffected by atmospheric noise.

Furthermore, closure phase can be used to recover uncontaminated source phase structure. In fact, the closure phase SNR is even more sensitively degraded by redundancy than the visibilities.[6] This is because the number of non-closing triangles (which give a random closure phase signal) climbs far more quickly than the small subset of closing triangles when redundancy is added to a pupil.

On the other hand, the Achilles heel of NRM, the limitation to bright targets, will be eliminated by the use of AO. In order to preserve fringe visibilities, NRM experiments are required to make integration times of the same order as the atmospheric coherence time, otherwise the fringes are washed out. Behind an AO system, the coherence time is effectively infinite, allowing arbitrarily long integrations to detect the fringes.

1.4. MTF (Visibility Calibration) Estimation from Telemetry

The calibration of traditional speckle imaging relies on sequentially sampling a calibrator point source, and the target of interest. The transfer function of the atmosphere and telescope is derived from the calibrator star, and used to rectify the target observations with Fourier deconvolution, assuming that the atmospheric properties have not changed between the two observations. Similar techniques have been attempted with conventional imaging AO, but with little success as the PSF has generally been found to vary too much between the target and calibrator.

Since AO systems operate in a null-seeking closed loop, the AO system is constantly measuring its own residual errors. In principle, these residuals can be used to reconstruct estimates of the system modulation transfer function (MTF) and hence PSF. This has been fairly successful with curvature AO,[11] but has not

yet been successfully implemented with Shack-Hartmann systems. These reconstructed PSFs rely on heuristic arguments and do not have the fidelity and credibility for accurate deconvolution.

In the case of a non-redundant mask, it is only necessary to retrieve the MTF amplitudes, and determine phases from closure methods. Thus, the WFS telemetry MTF estimate can be calibrated on a point source and applied to an observation, resulting in *simultaneous* visibility calibration, avoiding temporal fluctuations in the seeing as a calibration issue and avoiding the absolute calibration of the WFS telemetry for complete PSF reconstruction (see Figure 2).

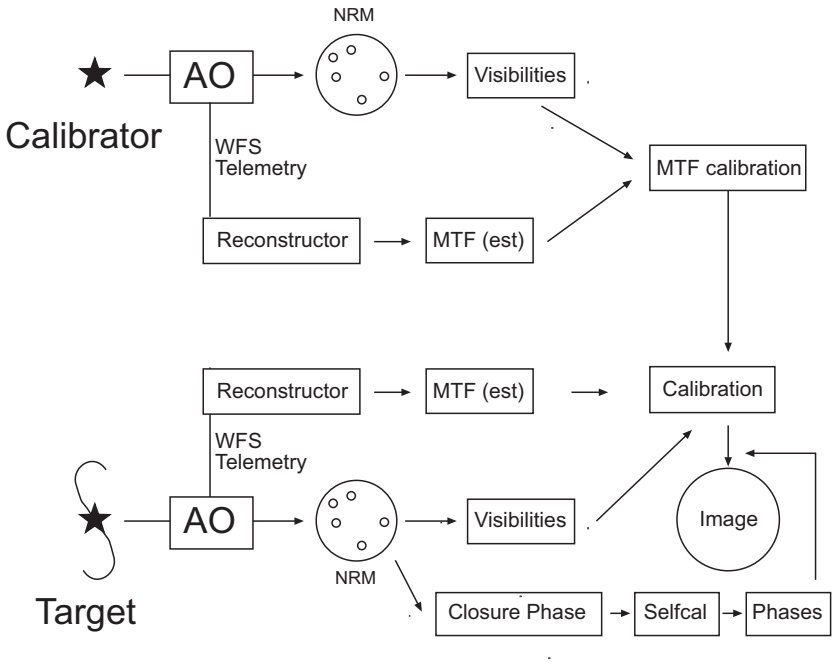

Figure 2. Data flow for calibration of non-redundant masking data. The wavefront sensor (WFS) telemetry data is used to estimate the MTF with methods similar to the Veran algorithm. This estimate is calibrated on a point source reference star. On the science target, the calibration is applied to the MTF reconstruction from WFS data and to produce calibrated visibilities and ultimately an image.

In summary, non-redundant masking combined with AO can deliver fainter limiting magnitudes than similar observations without AO, and precision PSF characterization resulting in higher dynamic range images than possible with either technique independently.

1.5. AO System Diagnostic Benefits

Masking interferometry provides a rich new set of observables to apply to AO system diagnostic problems. It is a unique property of a non-redundant aperture that fringes of a given spatial frequency in the interferogram can be associated with a single pair of subapertures in the pupil. This establishes a one-to-one mapping between the image plane and the deformable mirror, although only for that subset of the pupil which passes the mask. It should therefore be possible to establish precise causal relationships between the wavefront sensor/deformable mirror data and the output of the readout array. This has immediate application in, for example, the study of non-common path optical aberrations.

For purposes of measuring the AO system MTF, a masked aperture offers significant advantages over a filled aperture. Since the fringes are spread over many pixels the interferogram is of much lower dynamic range than

a filled pupil image, and is much more robust against many detector calibration issues such as background subtraction, flatfielding, linearity and bad pixels than traditional measures such a Strehl ratio obtained from filled pupil images. These advantages can be put to use in terms of providing differential MTF calibrations from AO system telemetry for science purposes. A comprehensive science program, applying this technique at multiple telescopes, will ultimately produce a large database of WFS telemetry data, estimated MTF reconstructions, and accurate MTF measurements as a byproduct of the necessary calibrations. These data will be highly valuable for identifying the relevant difficulties, and establishing a credible heritage for complete PSF reconstruction from AO telemetry data.

2. EXPERIMENTAL SETUP AND OBSERVATIONS

The implementation of sparse-aperture adaptive optics imaging requires only minor additions to an existing adaptive optics camera. A pupil image needs to be formed, at which a perforated opaque mask is placed. After the light propagates through a small number of carefully placed holes, an image is formed on a focal plane array detector (see Figure 3). Due to the narrow field of view and slow beams, the optical engineering requirements/tolerances are straightforward.

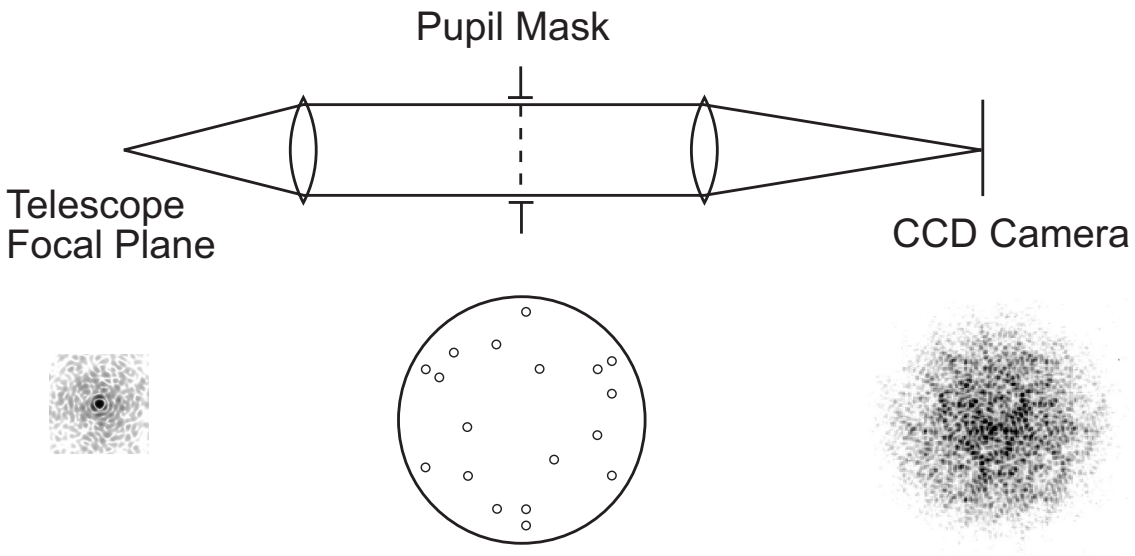

Figure 3. Optical layout required for sparse-aperture imaging. A pupil image is formed, at which an opaque mask with precision holes is placed. An image is formed and recorded with a CCD camera, through a filter. The resulting interferograms are processed with Fourier techniques.

2.1. Keck/Nirc2 experiments

Two masks have been fitted to the near-infrared Nirc2 camera which is operational downstream of the Keck 2 adaptive optics system. These masks, with 18-hole and 9-hole Golay-type non-redundant array layouts, were mounted in spare slots within two of the filter wheels of the camera. Note that this represents a significant advance over previous masking experiments at Keck,[7] both in terms of difficulty of running the experiment (masks mounted on the Keck secondary mirror needed to be installed by physically climbing onto the telescope structure during the observing night), and also in terms of elimination of thermal noise (the cryogenic temperature of the Nirc2 masks eliminates significant thermal background, as compared to the earlier dome-temperature masks).

With the relatively long (10 m) baselines available within the Keck aperture, our observational program has concentrated on astrophysical imaging targets. An example given here is the evolved mass-losing supergiant VY CMa, which earlier masking interferometry (without AO) has shown to possess a dramatic one-sided dust plume, as depicted in Figure 4 (upper panels). Further discussion and astrophysical interpretation can be found

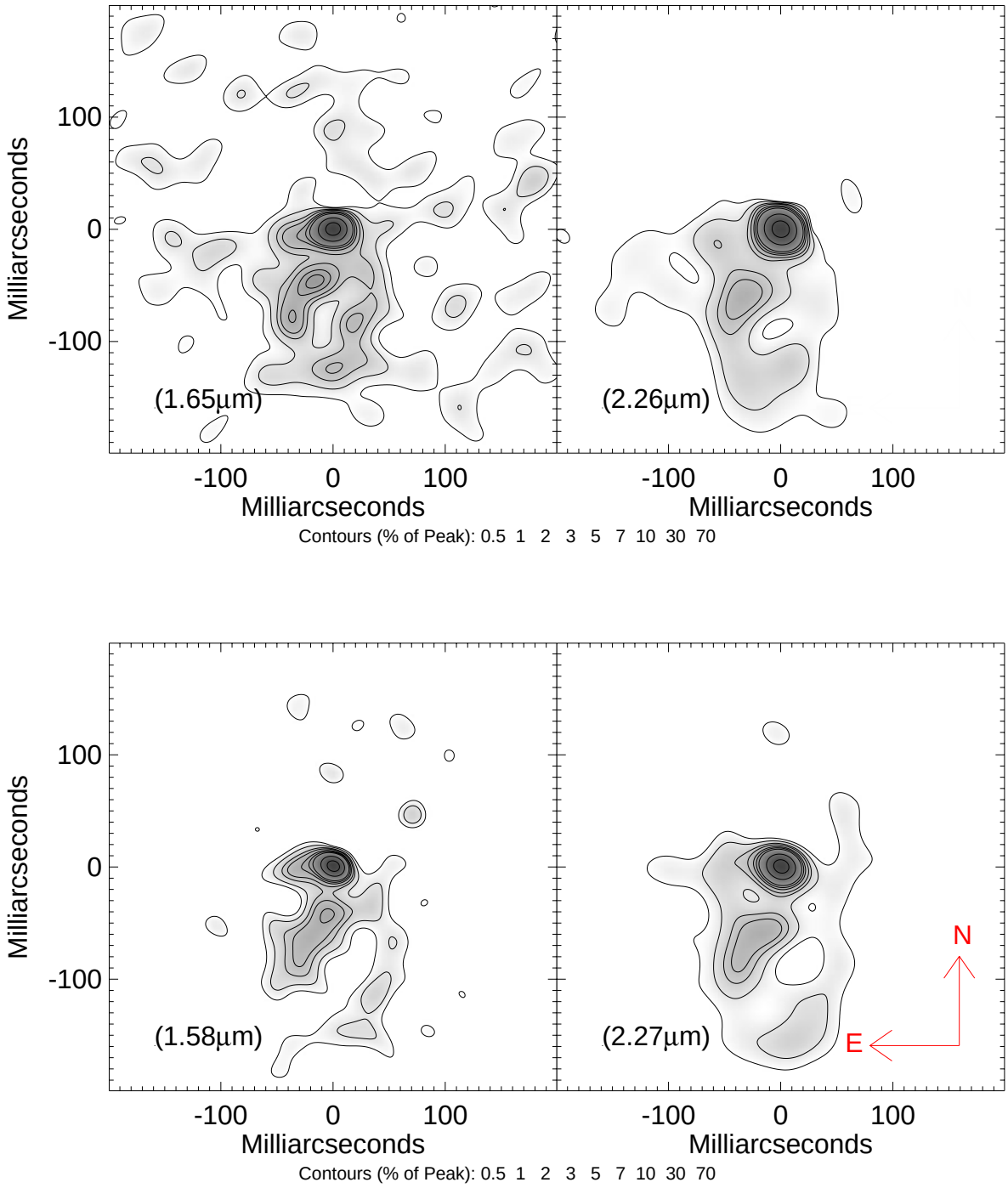

Figure 4. Images of the extreme mass-losing supergiant VY CMa. Upper panels show maps recovered from the earlier (seeing-limited) aperture masking experiment from data taken January 1997. Lower panels show images recovered with sparse-aperture AO from data taken in October 2005. Not only is it possible to demonstrate recovery of all the earlier features, but apparent motion of the dust plume is apparent over the ∼9 year interval since the original images. A detailed discussion with astrophysical interpretation of these images can be found in ref 12.

in ref 12; for the present we are interested in this object as a test case for our sparse-aperture AO imaging methodology.

Images recovered from sparse-aperture AO of the VY CMa system can also be found in Figure 4 (lower panels). Visual comparison of these images with those from the earlier masking program shows that real structures up to the full diffraction limit of the telescope have been recovered. Furthermore, an expansion of about 30mas for material in the outer dust plume can be reported over the elapsed observing time interval (a bit less than 9 years). Assuming a distance of 1.5Kpc to VY CMa, then 45 AU motion results in a computed outflow speed of ∼24 km/sec. This seems reasonable given the that this dust may be in the acceleration region (8.5 km/s increasing to 33 km/sec over 400 mas).

This demonstration-of-principle for sparse-aperture AO has shown recovery of structure from within a few resolution elements from the AO-corrected PSF. Furthermore, we have done so with only *ten frames* of AO-locked data, while earlier masking required hundreds of seeing-limited frames. Thus the Nirc2 aperture mask opens a new window of parameter space to diffraction-limited imaging: targets too faint for conventional masking, but with structures too near the core for reliable classical AO deconvolution.

2.2. Palomar/PHARO experiments

A program to explore precision calibration of AO images with the application of non-redundant aperture masking interferometry has been undertaken with the Mt Palomar 200-inch Adaptive Optics system.[13] In particular, this program has emphasized the detection of faint nearby companions within a few times λ/D of the core of the PSF – a region traditionally discarded by most coronagraphic technologies. Masks with 9 and 18 holes were fabricated and placed in the Lyot stop of the PHARO[14] camera. The hole positions were chosen so as to maximize Fourier coverage and transmission, while maintaining non-redundancy to preserve closure-phase.[6,15]

As an illustration, we select the example of the G 78-28 AB system,[16] an M3 dwarf with a companion detected in the astrometric Stellear Planet Survey (STEPS) program. G 78-28 was observed in four observing runs in

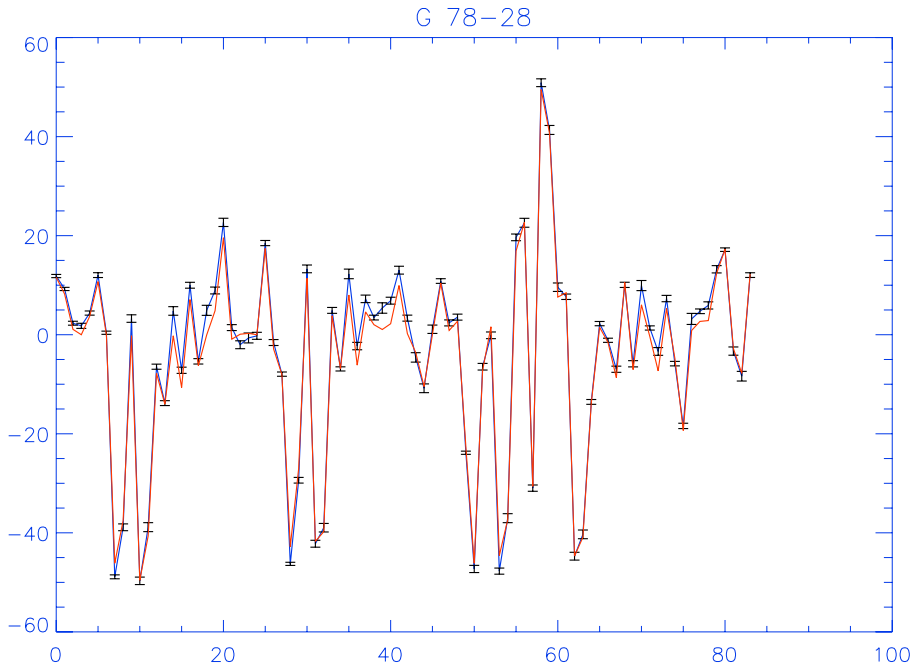

Figure 5. Closure-phase signals from observations of the close binary system G 78-28, plotted as an arbitrary ordering of the closing triangles. Overplotted is the predicted closure-phase signal from the best-fit binary model discussed further in the text.

December 2003, September 2005, December 2005 and February 2006. No fringes were detected in the September 2005 observations due to poor seeing. At V magnitude 12.4, G 78-28 is near the performance limit of the natural guide star AO system, requiring the AO system to operate at reduced bandwidth. The fringe stability is therefore a sensitive function of the atmospheric turbulence. Data were calibrated with observations of a nearby reference star, but care must be taken to select a source that is of similar brightness to both the AO wavefront sensor (operating in the red optical), and the science camera (operating in the infrared) to ensure compatibility.

The data were dark subtracted, flatfielded, and analysed with a custom software pipeline written in IDL. The pipeline outputs a bispectrum in OIFITS format.[17] A binary model could then be fit to the bispectrum. Although the binary signal is apparent in visibility amplitude through a power spectrum, in practice we have found that the visibility amplitude calibration is unreliable, and superior results are achieved with a fit to the closure phase alone. Presumably the visibility amplitude calibration remains more susceptible to fluctuations in seeing and AO performance between source and calibrator that plague conventional imaging with AO. For the observations reported here we neglect the visibility amplitude and the model is fit to the phase of the bispectrum. This is illustrated in Figure 5 which shows the closure phases recorded (ordered as an arbitrary numbering of the closing triangles) together with the best-fit model predictions. Median closure phase scatter were 3.5, 0.6 and 1.2 degrees in the Dec 2003, Sep 2005 and Feb 2006 data sets respectively. The Sep 2005 (JD 2453632.9) data set, is in the best seeing, and fortuitously the one in which the separation is largest. The reduced χ^2 of the bispectrum model fit is usually larger than one requiring a calibration error to be attributed to a systematic effect. The resulting final closure phase errors were 4.3, 2.0 and 1.2 degrees on the three datasets.

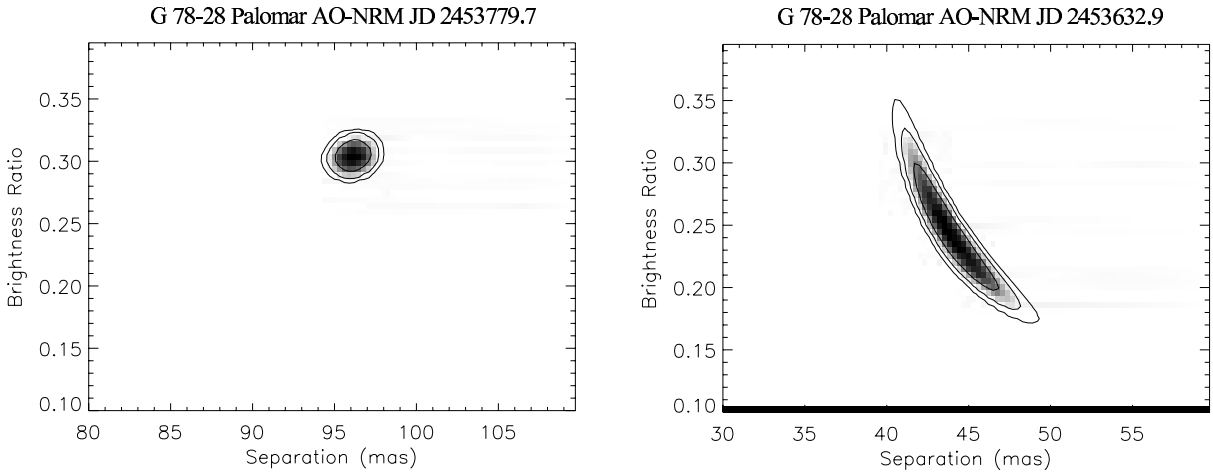

Figure 6. Likelihood contours for the best fit model to the binary system G 78-28 at two separate epochs. See text for further details.

The resulting extraction of astrometric parameters is a sensitive function of the orbital separation. In cases where the binary is well resolved, the solution is unambiguous (see Figure 6, left-hand panel). For the JD 2453779.7 observation the separation of 96 mas is well resolved (1.45 λ/D), and the resulting likelihood function is unambiguously fit with a unique separation and contrast. However, in the JD 2453632.9 observation, the separation is only 41 mas (0.62 λ/D). Even though well below the conventional "resolution limit" of the telescope, the binary is well detected, but there is degeneracy between the separation and contrast ratio. The shape of the likelihood contours shown in Figure 6 delineate regions of constant closure phase, which is proportional to the contrast ratio and ρ^4.

A nice demonstration of the final imaging precision obtained with sparse-aperture AO on the Palomar telescope is given in Figure 7. Errors on the orbital separation for the components of the G 78-28 binary system are dramatically reduced for the Palomar observations, as compared to radial velocity data and Keck laser guide star AO imaging. Further details and astrophysical interpretation of this system can be found in ref 16.

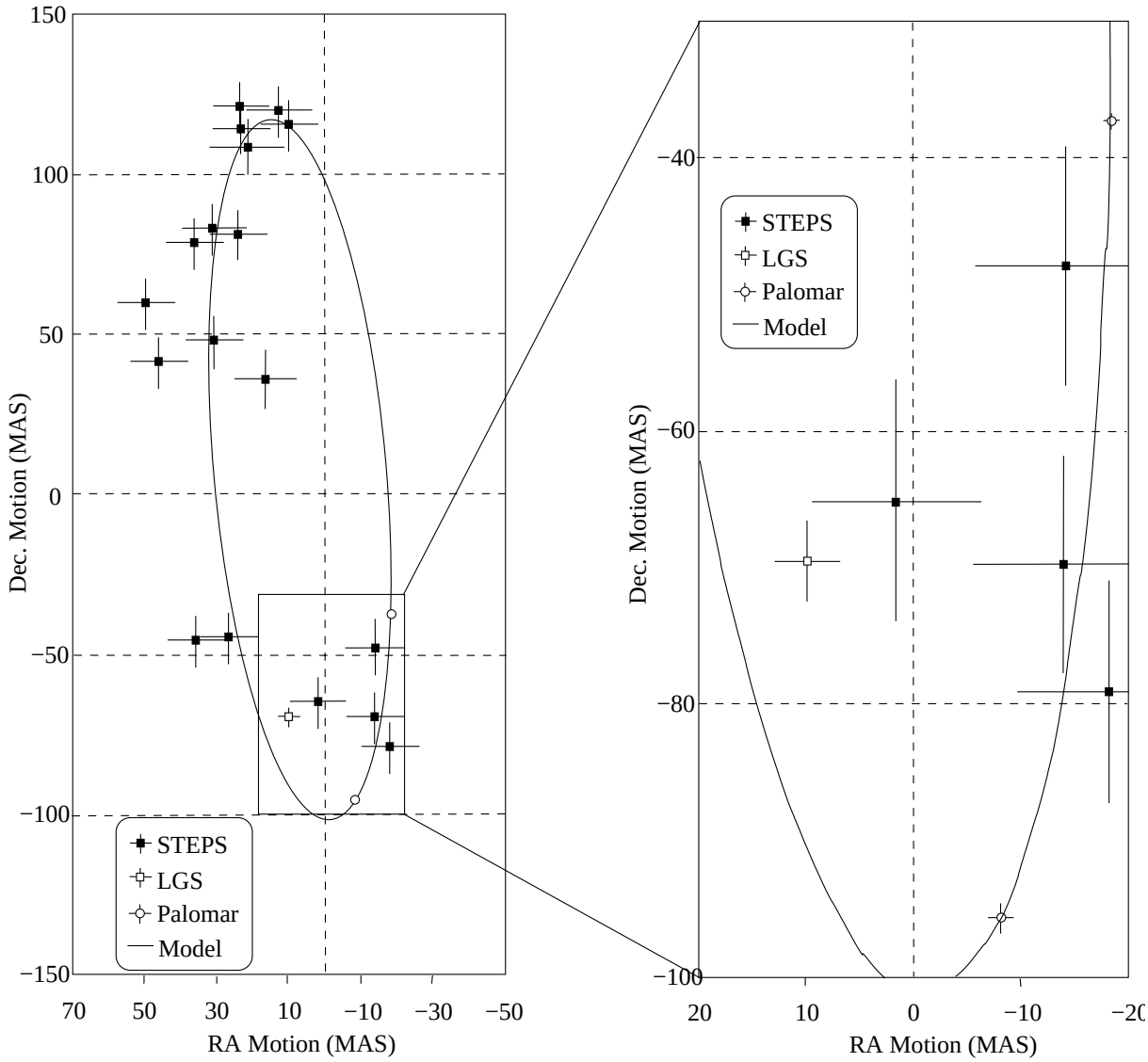

Figure 7. Orbital data on the binary system G 78-28 from the STEPS program, Palomar sparse-aperture AO, and a single data point from Keck laser guide star AO. The right-hand panel contains an enlargement of a region of the orbit containing the high-precision Palomar data points. A best-fitting orbit is overplotted as a solid line.

3. CONCLUSIONS

Sparse-aperture adaptive optics projects have been initiated at Keck and Palomar observatories. Performance in imaging targets exhibiting complex, asymmetric and extended structure, and also in detecting companions in the extremely close circumstellar environment has been demonstrated. The precision demonstrated in recovery of complex Fourier imaging data exceeds anything possible with simple deconvolution of the AO corrected PSF, lending observational weight to arguments that sparse-aperture techniques offer significant advantages for astrophysical imaging through the turbulent atmosphere.

REFERENCES

1. D. Apai, I. Pascucci, W. Brandner, T. Henning, R. Lenzen, D. E. Potter, A.-M. Lagrange, and G. Rousset, "NACO polarimetric differential imaging of TW Hya. A sharp look at the closest T Tauri disk," *Astr.*

Astrophys. **415**, pp. 671–676, Feb. 2004.
2. D. E. Potter, "A search for debris disks with a dual channel adaptive optics imaging polarimeter," *Ph.D. Thesis* , Nov. 2003.
3. M. D. Perrin, J. R. Graham, P. Kalas, J. P. Lloyd, C. E. Max, D. T. Gavel, D. M. Pennington, and E. L. Gates, "Laser Guide Star Adaptive Optics Imaging Polarimetry of Herbig Ae/Be Stars," *Science* **303**, pp. 1345–1348, Feb. 2004.
4. L. M. Close, R. Lenzen, J. C. Guirado, E. L. Nielsen, E. E. Mamajek, W. Brandner, M. Hartung, C. Lidman, and B. Biller, "A dynamical calibration of the mass-luminosity relation at very low stellar masses and young ages," *Nature* **433**, pp. 286–289, Jan. 2005.
5. C. Marois, R. Doyon, D. Nadeau, R. Racine, M. Riopel, P. Vallée, and D. Lafrenière, "TRIDENT: An Infrared Differential Imaging Camera Optimized for the Detection of Methanated Substellar Companions," *Publ. Astr. Soc. Pac.* **117**, pp. 745–756, July 2005.
6. A. C. S. Readhead, T. S. Nakajima, T. J. Pearson, G. Neugebauer, J. B. Oke, and W. L. W. Sargent, "Diffraction-limited imaging with ground-based optical telescopes," *Astron. J.* **95**, pp. 1278–1296, Apr. 1988.
7. P. G. Tuthill, J. D. Monnier, W. C. Danchi, E. H. Wishnow, and C. A. Haniff, "Michelson Interferometry with the Keck I Telescope," *Publ. Astr. Soc. Pac.* **112**, pp. 555–565, Apr. 2000.
8. J. E. Baldwin, C. A. Haniff, C. D. Mackay, and P. J. Warner, "Closure phase in high-resolution optical imaging," *Nature* **320**, pp. 595–597, Apr. 1986.
9. R. Racine, G. A. H. Walker, D. Nadeau, R. Doyon, and C. Marois, "Speckle Noise and the Detection of Faint Companions," *Publ. Astr. Soc. Pac.* **111**, pp. 587–594, May 1999.
10. A. Sivaramakrishnan, J. P. Lloyd, P. E. Hodge, and B. A. Macintosh, "Speckle Decorrelation and Dynamic Range in Speckle Noise-limited Imaging," *Astrophys. J. Lett.* **581**, pp. L59–L62, Dec. 2002.
11. J. P. Véran, F. Rigaut, H. Maître, and D. Rouan, "Estimation of the adaptive optics long-exposure point-spread function using control loop data," *Optical Society of America Journal* **14**, pp. 3057–3069, 1997.
12. J. D. Monnier, P. G. Tuthill, B. Lopez, P. Cruzalebes, W. C. Danchi, and C. A. Haniff, "The Last Gasps of VY Canis Majoris: Aperture Synthesis and Adaptive Optics Imagery," *Astrophys. J.* **512**, pp. 351–361, Feb. 1999.
13. M. Troy, R. G. Dekany, G. Brack, B. R. Oppenheimer, E. E. Bloemhof, T. Trinh, F. G. Dekens, F. Shi, T. L. Hayward, and B. Brandl, "Palomar adaptive optics project: status and performance," in *Proc. SPIE Vol. 4007, p. 31-40, Adaptive Optical Systems Technology, Peter L. Wizinowich; Ed.*, P. L. Wizinowich, ed., pp. 31–40, July 2000.
14. T. L. Hayward, B. Brandl, B. Pirger, C. Blacken, G. E. Gull, J. Schoenwald, and J. R. Houck, "PHARO: A Near-Infrared Camera for the Palomar Adaptive Optics System," *Publ. Astr. Soc. Pac.* **113**, pp. 105–118, Jan. 2001.
15. C. A. Haniff, C. D. Mackay, D. J. Titterington, D. Sivia, and J. E. Baldwin, "The first images from optical aperture synthesis," *Nature* **328**, pp. 694–696, Aug. 1987.
16. S. H. Pravdo, S. B. Shaklan, S. J. Wiktorowicz, S. Kulkarni, J. P. Lloyd, F. Martinache, P. Tuthill, and M. J. Ireland, "Masses of astrometrically discovered and imaged binaries: G78-28 ab and gj 232.1bc," *Astrophys. J. submitted* , 2006.
17. T. A. Pauls, J. S. Young, W. D. Cotton, and J. D. Monnier, "A Data Exchange Standard for Optical (Visible/IR) Interferometry," *Publ. Astr. Soc. Pac.* **117**, pp. 1255–1262, Nov. 2005.